The shell gland in laying and natural moulting commercial egg-type chickens: a histomorphological and ultrastructural study

M.-C. Madekurozwa* and M.M. Mpango

Department of Anatomy and Physiology, University of Pretoria, Private bag X04, Onderstepoort 0110, South Africa.

*Correspondence: Tel.: +27 12 529 8417; fax: +27 12 529 8320; e-mail: mary.madekurozwa@up.ac.za

Summary

The purpose of the present study was to determine the histological and ultrastructural changes in the luminal epithelium of the shell gland associated with natural moulting. Samples of the shell gland from laying (32 weeks old) and moulting (75 weeks old) hens were studied using histological, histochemical and electron microscopic techniques. In addition, TUNEL was used to demonstrate the distribution of apoptotic cells in the luminal epithelium of the shell gland. Autophagy, characterized by the presence of autophagosomes and autolysosomes was evident in the early stages of degeneration in non-ciliated, ciliated and mitochondrial cells. The intermediate and advanced stages of regression in non-ciliated, as well as mitochondrial cells occurred via apoptosis, while both apoptotic and necrotic ciliated cells were observed during the later stages of degeneration. The results of the present study suggest that a synergy of autophagy, apoptosis and necrosis is involved in the involution of the shell gland during natural moulting.

Keywords: Autophagy, apoptosis, necrosis, oviduct, electron microscopy, TUNEL, regression, involution.

Introduction

The shell gland has several functions which include: calcification of the egg shell (Yamamoto *et al.* 1985; Wasserman *et al*., 1991; Bar, 2009; Jonchere *et al*., 2012); “plumping”, which is the addition of water to the egg albumen (Wyburn *et al*., 1973); the production of shell matrix proteins (Hincke *et al*., 1995; Gautron *et al*., 2001ab; Fernandez *et al*., 2003); synthesis of the cuticle (Rahman *et al*., 2009; Wilson *et al*., 2017) and the deposition of pigments (Zhao *et al*., 2006; Hargitai *et al*., 2017).

The involution of the shell gland during moulting results in a decrease or cessation of the secretory processes occurring in this oviductal region (Yu and Marquardt, 1974; Williams and Ames, 2004). The cell death processes of apoptosis and necrosis have been shown to be involved in the regression of the shell gland during moulting (Heryanto *et al*., 1997). Apoptosis is known to culminate in the formation of apoptotic bodies composed of nuclear and cytoplasmic fragments (Kerr *et al.,* 1972; Sandow *et al*., 1979). These apoptotic bodies are subsequently phagocytosed by neighbouring epithelial cells or macrophages (Verhage *et al*., 1984; Sato *et al*., 1997; Elmore, 2007).

Necrosis had traditionally been regarded as a pathological condition triggered by cell injury (Fiers *et al*., 1999). However, subsequent research demonstrated the presence of a programmed form of necrosis, which operated in tandem with apoptosis (Zeiss, 2003; Edinger and Thompson, 2004). Indeed, research on oviductal involution during moulting has shown evidence of both apoptotic and necrotic cell death (Heryanto *et al*., 1997).

Extensive research has been conducted on the histology and ultrastructure of the shell gland in various avian species (Wyburn *et al*., 1973; Gupta and Maiti, 1987;

Chousalkar and Roberts, 2008; Madekurozwa, 2007, 2013, 2014). The majority of these studies have focussed on the shell gland in immature (Madekurozwa, 2007) or laying (Wyburn *et al*., 1973; Johnston *et al*., 1963; Breen and De Bruyn, 1969; Chousalkar and Roberts, 2008; Madekurozwa, 2013) birds, with relatively few studies being carried out on the histology of this oviductal region in moulting birds (Eroschenko and Wilson, 1974; Gupta and Maiti, 1987). Furthermore, there is currently a lack of published information on the ultrastructure of the shell gland in moulting birds.

Thus, the purpose of the present study was to investigate the histological and ultrastructural alterations in the luminal epithelium of the shell gland during natural moulting with a view to providing additional information on the modes of cell death involved in oviductal involution in the domestic fowl. A study of the shell gland in laying birds is included in order to establish a morphological baseline for comparison.

Materials and Methods

Animals and management

Twenty commercial egg layers (Hy-line W36) were utilized in this study. This type of chicken reaches peak production at 32 weeks, while natural moulting commences at 65-75 weeks of age (Hy-line W36 commercial layers management guide 2016). Ten 32-week-old laying and ten 75-week-old natural moulting hens were selected. The moulting birds were known to have ceased egg production for 7 days. Laying and moulting hens were obtained from the same commercial farm, but were maintained in separate poultry houses. All birds were fed layers mash and maintained under a light regime of 16h light: 8 h dark from 30 weeks of age as recommended by the breeder company. The birds were killed by decapitation. All the procedures used in this study

were approved by the Animal Ethics Committee of the University of Pretoria (approval number AEC V002/17).

Necropsy

The oviduct was cut longitudinally to expose the luminal surface of the organ and the position, as well as the developmental stage of the forming egg in the oviduct was noted. Developing eggs were present in the oviducts of all laying birds. Eggs were situated in the shell gland regions of the oviducts in four of the ten laying birds. No eggs were present in the oviducts of the moulting birds. Tissue samples were collected from the middle region of the shell gland.

Light microscopy

Samples for light microscopy were fixed in 10% buffered neutral formalin for 5 days. The tissue samples were then processed routinely for light microscopy. Tissue sections (5μm thick) were mounted on glass slides and stained with haematoxylin and eosin, Alcian blue (Alcian blue stain kit pH2.5, ab150662, Abcam), as well as Periodic Acid Schiff (Periodic acid Schiff stain kit, ab150680, Abcam) with and without diastase treatment.

Terminal deoxynucleotidyl transferase (TdT)- mediated deoxyuridine 5'-triphosphate (dUTP) nick-end labelling (TUNEL)

Apoptotic cells were detected using the TUNEL assay. The technique was performed on 5 μm thick sections using an ApopTag plus peroxidase *in situ* apoptosis

detection kit (Millipore, Temecula, USA) following the manufacturer's instructions. Sections were deparaffinized, rehydrated through a graded series of ethanol and washed in 0.01M phosphate buffered saline solution (PBS, pH 7.4). The sections were then pretreated with proteinase K (20μg/ml) for 15 min at room temperature. The slides were then rinsed in two changes of distilled water for 2 min each. Endogenous peroxidase activity was blocked using a 3% (v/v) hydrogen peroxidase solution in PBS for 5 min. The slides were then rinsed in PBS for 5 min. Thereafter, the sections were incubated with an equilibration buffer (ApopTag plus peroxidase kit, Millipore, Temecula, USA) at room temperature for 10 min. Excess buffer was tapped off the sections before the application of working strength TdT enzyme (77μl reaction buffer and 33μl TdT enzyme). The sections were then incubated in a humidified chamber at 37^0C for 1h. The reaction was stopped by rinsing the sections in stop/wash buffer (ApopTag plus peroxidase kit, Millipore, Temecula, USA) for 10 min at room temperature. The sections were then rinsed in three changes of PBS for 1 min each. The excess buffer was tapped off before the application of anti-digoxigenin conjugate (ApopTag plus peroxidase kit, Millipore, Temecula, USA). The sections were then incubated in a humidified chamber for 30 min at room temperature. The sections were then rinsed in four changes of PBS for 2 min each. Excess buffer was then tapped off the slides. Apoptotic nuclei were visualized after the addition of a diaminobenzidine solution (ApopTag plus peroxidase kit, Millipore, Temecula, USA). The sections were then rinsed in distilled water and counterstained with 0.5% (w:v) methyl green for 10 min at room temperature. The slides were then rinsed in distilled water and then dehydrated in 100% N-butanol and cleared in xylene.

In the negative controls TdT enzyme reagent was replaced with distilled water. Rat mammary gland (supplied with the ApopTag plus peroxidase kit) was used as a positive control.

The number of TUNEL positive nuclei in 100μm lengths of epithelium in 15 random microscopic fields per bird were counted with the aid of an image analyzer system (CellSens dimension software) connected to an Olympus BX-63 microscope.

Statistical analysis

TUNEL positive nuclei counts in laying and moulting hens were analyzed with the Independent samples t-test using IBM SPSS version 25 software. A P value of <0.05 was considered to be statistically significant.

Scanning electron microscopy (SEM)

The SEM procedure was carried out as previously described (Madekurozwa, 2007). In brief, tissue samples for SEM were pinned flat, rinsed in 0.075M phosphate buffer (pH 7.4) and then fixed in buffered 2.5% glutaraldehyde. After fixation the samples were rinsed in phosphate buffer, and post-fixed in 0.5% aqueous osmium tetroxide. The samples were then washed with double-distilled water, dehydrated in a graded series of ethanol before being dried in a critical point chamber with liquid CO_2. The samples were then mounted using conductive silver paint, sputter-coated with gold and viewed using a Zeiss Crossbeam 540 FEG scanning electron microscope operated at 3kv.

Transmission electron microscopy (TEM)

The TEM procedure was conducted as described in a previous study (Madekurozwa, 2007). Tissue samples were immersion-fixed in 2.5% glutaraldehyde in 0.075M phosphate buffer (pH 7.4) for 24 hours. Thereafter, the tissue samples were rinsed with phosphate buffer (pH 7.4) and post-fixed in 0.5% osmium tetroxide for 2 hours. The tissue samples were then washed with ddH_2O, dehydrated in a graded series of ethanol concentrations, followed by a propylene oxide rinse and infiltrated with a propylene oxide:epoxy resin mixture at a ratio of 1:2 for 1 hour, 1:1 for 2 hours and 100% resin overnight. The samples were then polymerized in fresh 100% resin for 24 hours at 60°C. Semi-thin (350nm) sections were cut and stained with toluidine blue. Ultra-thin (90nm) sections were cut using a diamond knife, and subsequently stained with lead acetate and uranyl citrate. The samples were viewed with a Philips CM10 transmission electron microscope (FEI, The Netherlands), fitted with an Olympus Mega View III imaging system.

Results

Histomorphology of the luminal epithelium

The tunica mucosa of the shell gland in laying was arranged in slender, long primary folds which gave rise to short secondary folds. Lining the folds was a pseudostratified columnar epithelium, which comprised of non-ciliated and ciliated cells (Fig. 1a). The regressing luminal epithelium in moulting birds contained cells with vacuolated cytoplasm and occasional dark-staining nuclei (Fig. 1b).

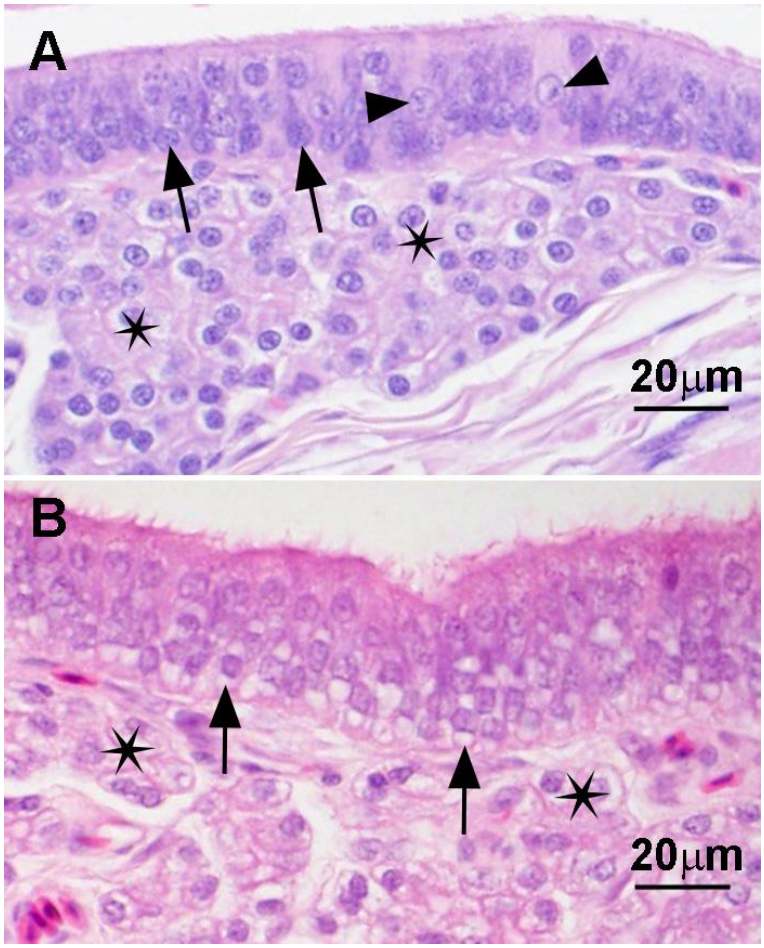

Figure 1. Light photomicrographs of the shell gland in laying (A) and moulting (B) birds. Haematoxylin and eosin-stained sections. **A**. Arrows: nuclei of non-ciliated cells. Arrowheads: nuclei of ciliated cells. Asterisks: tubular glands. **B**. Arrows: cells with cytoplasmic vacuoles. Asterisks: tubular glands.

Ciliated cells in laying birds were periodic acid Schiff negative, while diastase-resistant, magenta-coloured periodic acid Schiff positive material was demonstrated in the supranuclear and infranuclear regions of non-ciliated cells (Fig. 2a).

Non-ciliated cells contained diastase-resistant periodic acid Schiff positive material during the early and intermediate stages of regression. Vacuolated periodic acid Schiff positive cytoplasm was observed in non-ciliated cells during the advanced stages of regression (Fig. 2b).

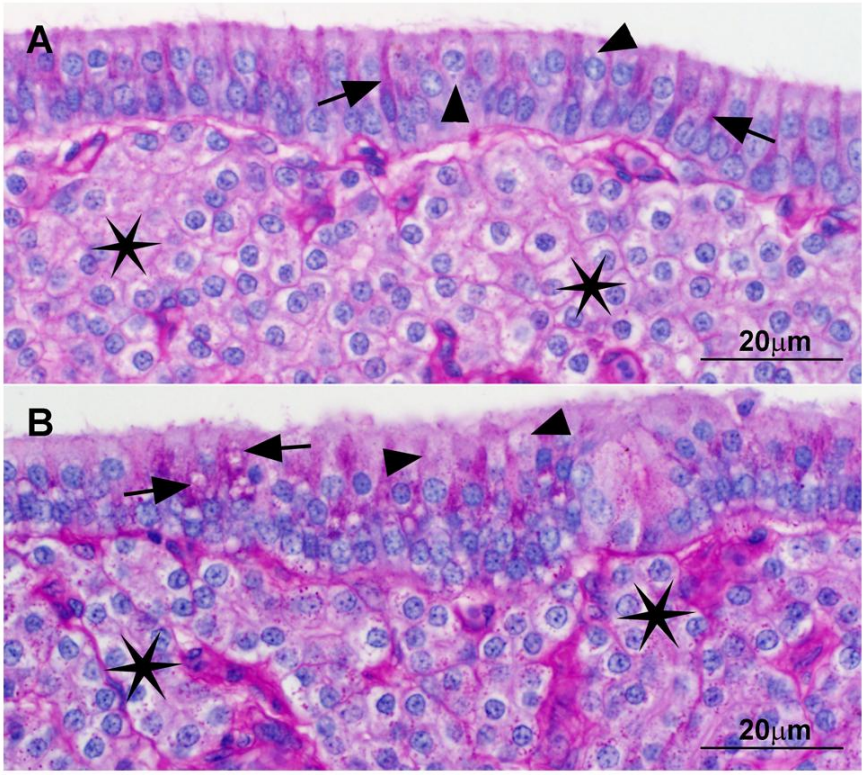

Figure 2. Light photomicrographs of the shell gland in laying (A) and moulting (B) birds. Periodic-acid Schiff (PAS)-stained sections. **A**. Luminal epithelium with PAS positive non-ciliated cells (arrows) and PAS negative ciliated cells (arrowheads). Asterisks: tubular glands. **B**. PAS-staining in the vacuolated cytoplasm of non-ciliated cells (arrows). Arrowheads: ciliated cells. Asterisks: tubular glands.

The luminal epithelium in laying and moulting birds was Alcian blue negative.

Demonstration of apoptotic cells using the TUNEL technique

TUNEL-staining in the shell gland luminal epithelium of laying birds was negligible (Fig. 3a). The nuclei of luminal epithelial cells in moulting birds were predominantly TUNEL-positive (Fig. 3b). A few viable nuclei, which were methyl green-stained, were seen among the TUNEL-positive apoptotic nuclei (Fig. 3b). No TUNEL-stained nuclei were observed in the negative control sections (Fig. 3c).

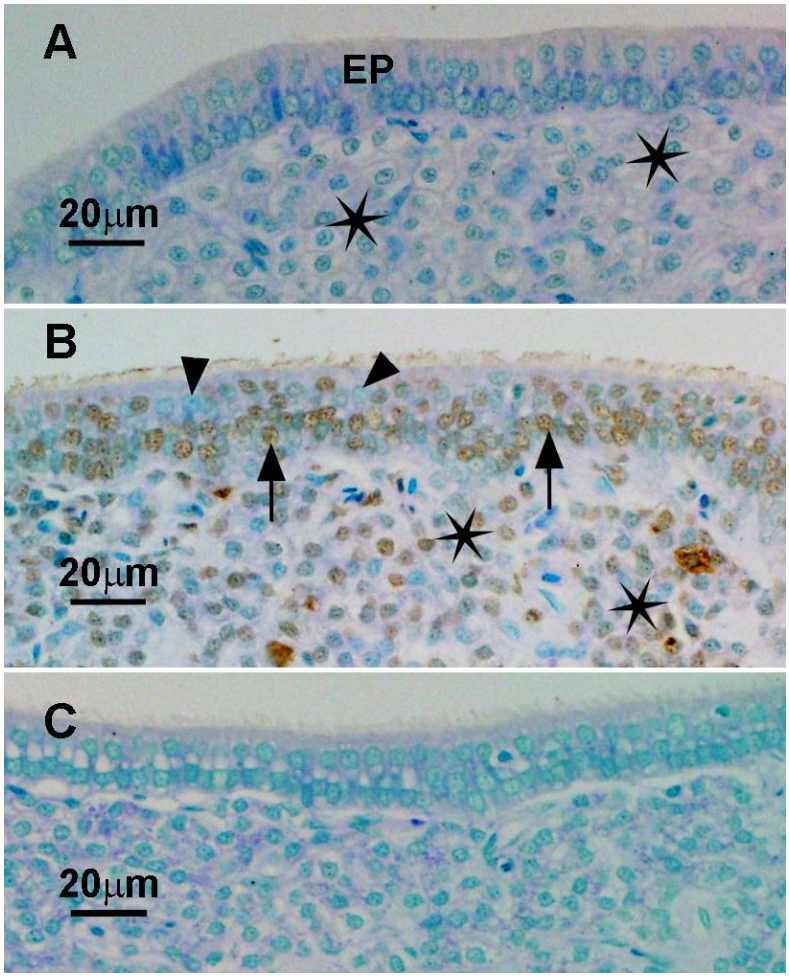

Figure 3. TUNEL (TdT-mediated dUTP nick end labelling) stained sections of the shell gland in laying (A) and moulting (B-C) birds. **A**. EP: TUNEL-negative epithelium. Asterisks: tubular glands. **B**. Apoptotic (arrows) and viable (arrowheads) nuclei in the luminal epithelium. **C**. Negative control section.

The mean +/- standard deviation of TUNEL-positive cells in laying birds was 0.4 +/- 0.69 (N = 10), and 27.7 +/- 3.83 (N = 10) for moulting birds. The standard error mean was 0.22 for laying birds and 1.21 for the moulting birds. The results of the Independent samples t-test revealed a significant difference between the mean counts of TUNEL-positive cells in laying and moulting hens. The mean difference in TUNEL cell counts was 27.3, while the standard error difference was 1.23 at a 95% confidence

interval. In summary the number of apoptotic nuclei was significantly higher in moulting birds compared to laying hens.

Scanning electron microscopic study of the luminal surface

Non-ciliated and ciliated cells lined the luminal surface of the shell gland in laying birds. The non-ciliated cells were dome-shaped and covered with microvilli. The ciliated cells were lined by microvilli and cilia, the latter of which partially obscured adjacent non-ciliated cells (Fig. 4a).

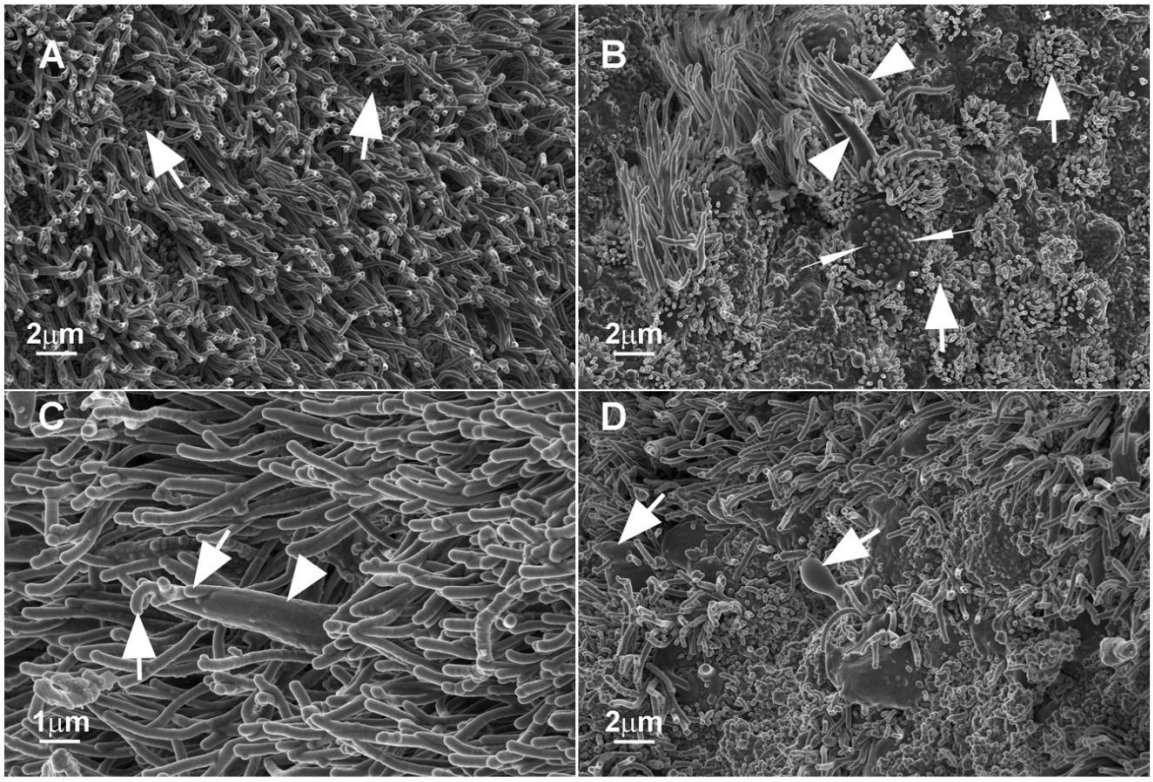

Figure 4. Scanning electron photomicrographs of the shell gland in laying (A) and moulting (B-D) birds.

A. Microvilli-covered non-ciliated cells (arrows) among ciliated cells. **B**. Short microvilli (thin arrows) line a non-ciliated cell. Thick arrows: deciliated cells covered with microvilli. Arrowheads: cilia packets.

C. Cilia (arrows) within a cilia packet (arrowhead). **D**. Irregular-shaped protrusions (arrows) extend from sparsely ciliated cells.

The surfaces of non-ciliated cells in moulting birds were covered by a few short microvilli (Fig. 4b). In addition, non-ciliated cells with disrupted apical plasma membranes were occasionally observed. Cilia packets and deciliation were the main morphological degenerative changes involving ciliated cells (Fig. 4b & c). In addition, irregular-shaped cytoplasmic protrusions extended from sparsely-ciliated cells (Fig. 4d).

Transmission electron microscopic study of the luminal epithelium

Non-ciliated, ciliated and mitochondrial cells formed the luminal epithelium of the shell gland in laying and moulting birds. Nuclei in non-ciliated and mitochondrial cells were placed basally, while those of the ciliated cells were situated in the apical or middle regions of the cells (Fig. 5a).

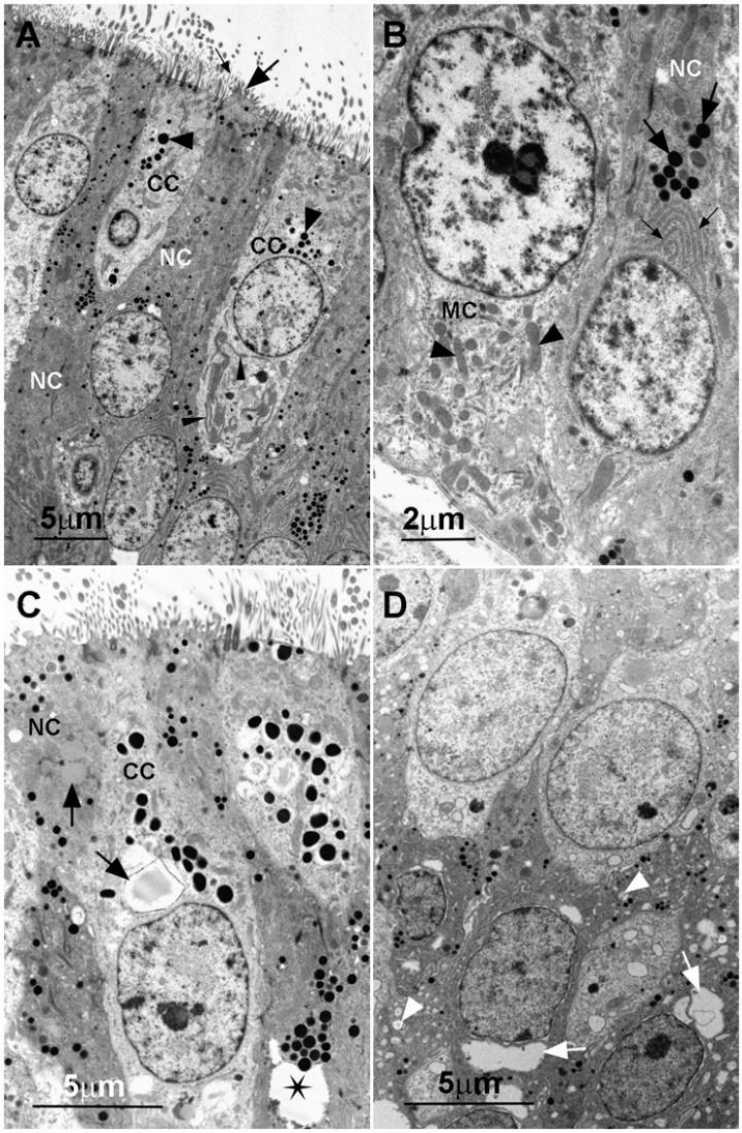

Figure 5. Transmission electron photomicrographs of the shell gland luminal epithelium in laying (A-B) and moulting (C-D) birds. **A**. Electron dense non-ciliated (NC) and electron lucent ciliated (CC) cells form the luminal epithelium. Thick (thick arrow) and thin (thin arrow) microvilli line non-ciliated and ciliated cells respectively. Accumulations of secretory granules (thick arrowheads) and RER cisternae (thin arrowheads) are observed in the ciliated cells. **B**. NC: non-ciliated cell containing a mass of secretory granules (thick arrows) and profiles of RER (thin arrows). MC: mitochondrial cell with numerous mitochondria (arrowheads). The nucleus of the mitochondrial cell contains an aggregation composed of multiple nucleoli (asterisk). **C**. Lipid droplet autophagosomes (arrows) in non-ciliated (NC) and ciliated (CC) cells. Arrowheads: groups of secretory granules in close proximity to a vacuoloid (asterisk). **D**. Vacuoloids (arrows) and dilated RER cisternae (arrowheads) in degenerating non-ciliated cells.

Non-ciliated cells

The apical plasma membranes of non-ciliated cells in laying birds displayed tufts of thick microvilli (Fig. 5a). Secretory granules (0.21 μm to 0.44 μm in diameter) and elongated mitochondria were evenly distributed throughout the supranuclear cytoplasm of non-ciliated cells. In addition, the area immediately above the nucleus contained an accumulation of secretory granules, which was associated with stacked profiles of rough endoplasmic reticulum (RER) (Fig. 5b).

The occurrence of lipid droplet autophagosomes in the supranuclear cytoplasm was a noteworthy feature during the early stages of involution in non-ciliated cells of moulting birds (Fig. 5c). The lipid droplet autophagosomes were typically observed closely associated with secretory granules. Non-ciliated cells in the intermediate stages of degeneration contained: condensed nuclei with prominent perinuclear spaces; swollen mitochondria; infranuclear and supranuclear vacuoloids, as well as dilated RER cisternae (Fig. 5c & d). The vacuoloids were associated with masses of degenerating secretory granules (Fig. 5c), and occasionally with RER cisternae. Upon dissolution the disintegrating secretory granules left clear spaces which were incorporated into the vacuoloids.

In the advanced stages of regression, attenuated regions of cytoplasm connected the proximal and distal parts of degenerating non-ciliated cells (Fig. 6a). The eventual separation of the proximal and distal segments of the non-ciliated cells resulted in the formation of proximally-located cytoplasmic fragments (Fig. 6b) and distally-situated apoptotic bodies (Fig. 6c). The apoptotic bodies were composed of intact or fragmented nuclei enclosed in cytoplasm.

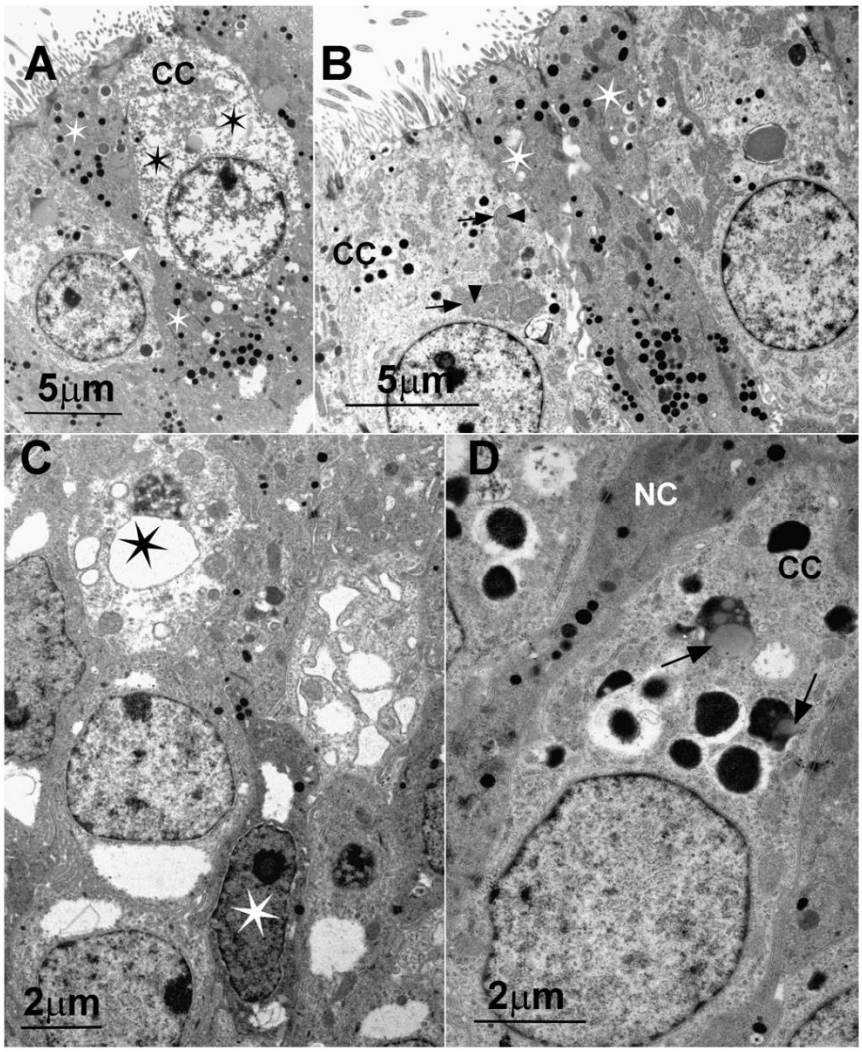

Figure 6. Transmission electron photomicrographs of the shell gland luminal epithelium in moulting birds. **A**. Proximal and distal regions (white asterisks) of a regressing non-ciliated cell are connected by a constricted region of cytoplasm (arrow). The neighbouring electron lucent ciliated cell (CC) contains numerous clear spaces (black asterisks). **B**. Asterisks: disconnected apical regions of non-ciliated cells. RER cisternae (arrows) encircle disintegrating mitochondria (arrowheads) in the adjacent degenerating ciliated cell (CC). **C**. Apoptotic bodies formed from non-ciliated (white asterisk) and ciliated (black asterisk) cells. **D.** Degenerating secretory granules containing lipid droplets (arrows). CC: ciliated cell. NC: non-ciliated cell.

Ciliated cells

The apical plasma membranes of ciliated cells in laying birds exhibited uniformly-arranged cilia interspersed with long, thin microvilli (Fig. 5a) Contained within the sub-luminal cytoplasm were numerous mitochondria and a few electron dense bodies (0.27 μm to 0.35 μm in diameter). Large pleomorphic secretory granules (0.80 μm to 1.05 μm in diameter), a few RER cisternae, ribosomes and a prominent Golgi complex occupied the supranuclear area. A large, round, euchromatic nucleus with a few clumps of chromatin was present. The infranuclear region contained mitochondria and long RER cisternae (Figure 5(a)). Occasional secretory granules were observed in the infranuclear area.

The early stages of degeneration in ciliated cells were characterized by the presence of disintegrating mitochondria which were partially or totally enclosed in RER cisternae (Fig. 6b). In addition, ciliated cells in the initial stages of involution contained autophagosomes, autolysosomes, as well as degenerating secretory granules. Lipid droplets of various sizes were also observed in degenerating secretory granules (Fig. 6d).

Ciliated cells with electron dense and electron lucent cytoplasm were observed during the intermediate and late stages of regression (Fig. 7a). Apically the electron dense cells displayed broad, irregular-shaped cytoplasmic processes (Fig. 7a). In addition, deciliation via the formation of cilia packets was observed in the degenerating electron dense cells (Fig. 7b). The cilia packets were formed by clumps of cilia which were surrounded by a plasma membrane. The supranuclear cytoplasm of regressing electron dense ciliated cells contained: a few circular profiles of RER; degenerating secretory granules; Golgi complexes with dilated tubules, and swollen mitochondria

(Fig. 7a). The irregular-shaped nuclei of these cells displayed chromatin aggregation and margination (Fig. 7a).

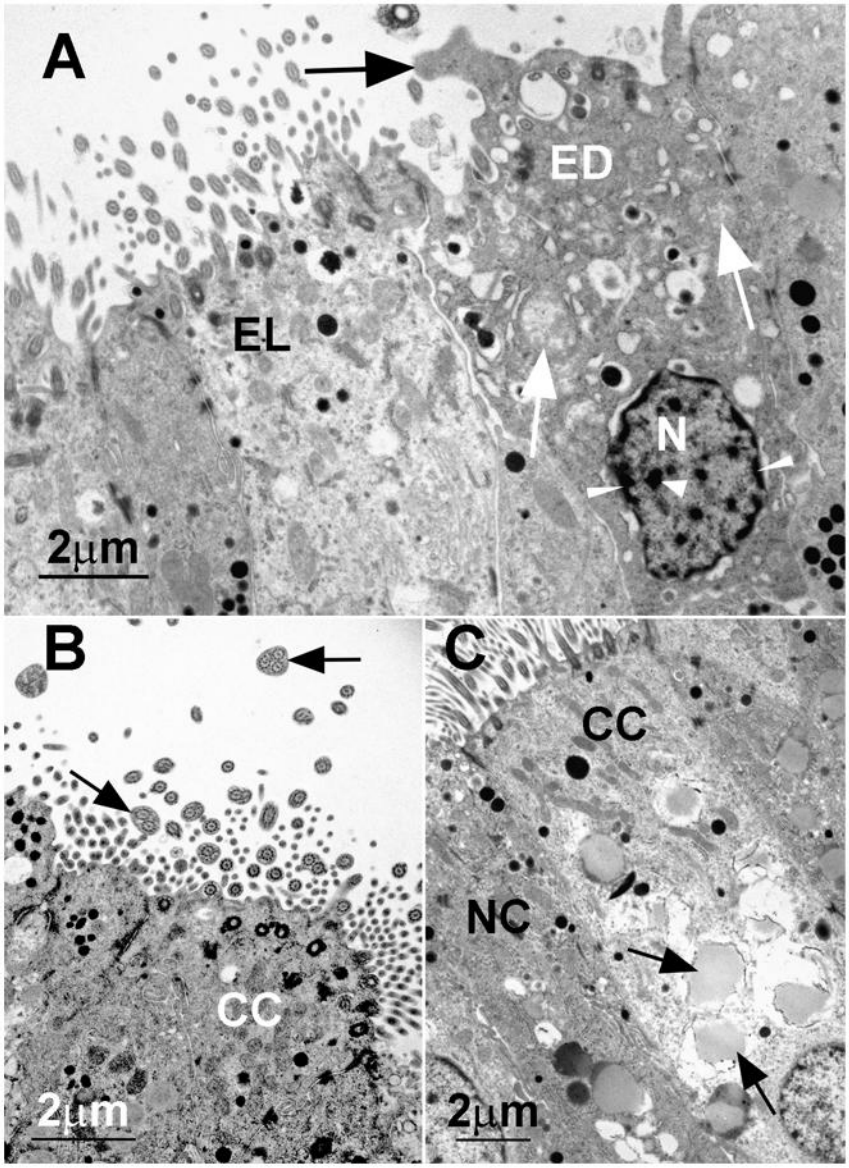

Figure 7. Transmission electron photomicrographs of the shell gland luminal epithelium in moulting birds. **A**. Degenerating electron lucent (EL) and electron dense (ED) ciliated cells. An irregular-shaped cytoplasmic protrusion (black arrow) extends from the electron dense ciliated cell. White arrows: swollen mitochondria. N: nucleus displaying chromatin aggregation (thick arrowhead) and margination (thin arrowheads). **B**. Ciliary packets (arrows) contain two or three cilia enclosed in a plasma membrane. CC: ciliated cell. **C**. Disintegrating lipid droplet autophagosomes (arrows) in a degenerating electron lucent ciliated cell (CC). NC: non-ciliated cell.

As mentioned previously, electron dense and electron lucent ciliated cells occurred during the intermediate and late stages of degeneration. During the intermediate stage of regression, the electron lucent ciliated cells typically contained: numerous vacuoles; dilated RER profiles; swollen mitochondria; electron dense bodies and degenerating secretory granules. Additionally, the presence of disintegrating lipid droplet autophagosomes was a major feature of some degenerating electron lucent ciliated cells (Figs. 5c & 7c). The lipid droplet autophagosomes were larger than those observed in non-ciliated cells.

The dissolution of lipid droplets and secretory granules during the advanced regressive stages in electron lucent ciliated cells resulted in a preponderance of clear spaces throughout the cytoplasm (Fig. 6a). In addition, the formation of apoptotic bodies was a notable feature during this stage of involution. The apoptotic bodies comprised of nuclear fragments enclosed in cytoplasm (Fig. 6c). Disintegrating organelles were contained within the cytoplasm.

Mitochondrial cells

Mitochondrial cells in the shell gland of laying birds were typically elongated in shape. The apical regions of the cells exhibited single or multiple broad cytoplasmic protrusions. The mitochondrial cells contained irregular-shaped, euchromatic nuclei with multiple nucleoli (Fig. 5b). Numerous mitochondria with distinct cristae dominated the cytoplasm (Fig. 5b). Interspersed between the mitochondria were short profiles of RER, bundles of fibrils and ribosomes.

Mitochondrial cells undergoing early and intermediate stages of regression variably contained autophagosomes, lysosomes, autolysosomes and multivesicular bodies (Fig. 8a). In the advanced stages of degeneration mitochondrial cells were characterized by the presence of swollen mitochondria, condensed cytoplasm, electron dense nuclei, and basally-located vacuoles (Fig. 8b).

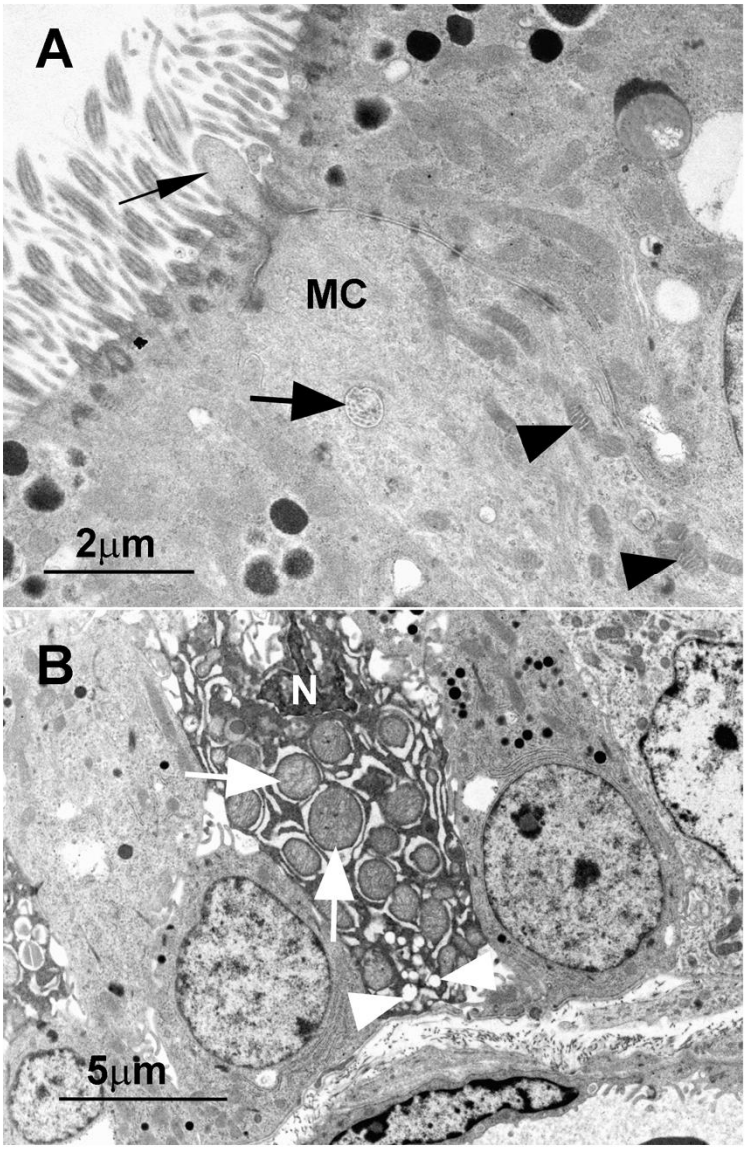

Figure 8. Transmission electron photomicrographs of the shell gland luminal epithelium in moulting birds. **A**. A multivesicular body (thick arrow) in a mitochondrial cell (MC). Thin arrow: cytoplasmic protrusion. Arrowheads: mitochondria with distinct cristae. **B**. Condensed nucleus (N), swollen mitochondria (arrows) and vacuoles (arrowheads) in a degenerating mitochondrial cell.

Discussion

Non-ciliated cells

Periodic-acid Schiff-alcian blue (PAS-Ab) positive staining, which was indicative of the presence of both acidic and neutral mucopolysaccharides, was demonstrated in the cytoplasm of non-ciliated cells in the shell glands of laying birds. This result is in agreement with the findings of previous studies on commercial egg layers (Robinson *et al*., 1968; Breen and De Bruyn, 1969). In the present study on Hy-line W36 hens, the location of the PAS-Ab positive material coincided with the position of electron dense secretory granules observed using the transmission electron microscope. In the current investigation the PAS-Ab negativity of non-ciliated cells during the late degenerative stages coincided with the disintegration of secretory granules and the replacement of these inclusions by vacuoloids. The occurrence of prominent supranuclear and infranuclear vacuoloids was a noteworthy feature of degenerating non-ciliated cells in the current study. Infranuclear and supranuclear vacuoloids have been observed in non-ciliated cells of the shell gland in Thornber 505 hybrid (Johnston *et al.,* 1963) and white leghorn (Breen and De Bruyn, 1969) domestic fowls. In addition, similar structures have been reported in non-ciliated shell gland cells in the Japanese quail (Yamamoto *et al*., 1985). Interestingly, in the current investigation on Hy-line W36 hens, large supranuclear and infranuclear vacuoloids were only observed in the non-ciliated cells of moulting birds. The reason for the discrepancy in the results of the current study and the findings of previous investigations on the domestic fowl (Johnston *et al.,* 1963; Breen and De Bruyn, 1969) and Japanese quail (Yamamoto *et al*., 1985) is unclear.

In the current investigation the presence of lipid droplet autophagosomes was indicative of autophagy, while the formation of apoptotic bodies was a characteristic

end stage of apoptosis. The formation of apoptotic bodies, via the processes of constriction and eventual separation, has also been reported in non-ciliated cells in the postovulatory oviduct of the cat (Verhage *et al*., 1984). It is known that apoptotic bodies are rapidly phagocytosed by neighbouring epithelial cells or macrophages (Kerr *et al*., 1972; Sato *et al*., 1997). However, the fate of apoptotic bodies in the current study was unclear. According to Kerr *et al*. (1972), apoptotic bodies are rapidly phagocytosed and degraded. Thus, the failure to observe phagocytosed apoptotic bodies in the current study may be due to the rapidity of the digestive process.

Ciliated cells

The morphological and ultrastructural appearance of ciliated cells in the present study was in agreement with the findings of previous studies on Thornber hybrid (Johnston *et al*., 1963) and white leghorn hens (Breen and De Bruyn, 1969). In contrast to similar cells in the oviduct, ciliated cells in the shell gland contain secretory granules. In the current investigation the secretory granules were PAS-Ab negative, suggesting an absence of mucopolysaccharides in these cells. Similar findings have been reported in white leghorn hens (Breen and De Bruyn, 1969).

In the current study, electron dense bodies were observed in the apical cytoplasm of ciliated cells in laying birds. These bodies were morphologically distinct from the large supranuclear secretory granules. A study by Breen and De Bruyn (1969) reported the presence of lysosome-like bodies in the apical cytoplasm of ciliated cells during the formation of the egg shell. However, the function of these lysosome-like bodies is currently unclear. Thus, further studies are required to determine the exact

nature and function of these electron dense bodies in the ciliated cells of the shell gland in laying birds.

In present investigation autophagy occurred during the early degenerative stages of ciliated cells in moulting birds. Whereas the findings of the present study appear to be the first report of autophagy in the regressing shell gland, this degenerative process is known to be involved in the involution of the uterus in the hamster (Sandow *et al*., 1979), rat (Spornitz *et al*., 1994) and opossum (Wick and Kress, 2002). The encirclement of mitochondria by RER cisternae, as well as the presence of autophagosomes and autolysosomes were typical features of autophagy in the present study. Although the exact mechanisms involved in autophagy are still unclear, it is known that RER contributes to the formation of the membranes enclosing the autophagosome (Biazik *et al*., 2015; Sanchez-Wandelmer *et al*., 2015).

In the present study degenerating electron dense and electron lucent ciliated cells were observed during the intermediate and late stages of shell gland involution. The electron dense cells exhibited characteristics of apoptosis, while necrotic changes were identified in the electron lucent ciliated cells. The occurrence of apoptosis and necrosis during the involution of the shell gland has previously been reported in commercial egg layers (Heryanto *et al*., 1997). The study by Heryanto *et al*. (1997) utilized TUNEL and acid phosphatase histochemistry to detect apoptosis and necrosis, respectively. In the present study apoptotic and necrotic cells in the shell gland were differentiated using electron microscopy, with the further application of TUNEL to exhibit the distribution of cells undergoing apoptosis. The use of transmission and scanning electron microscopy in the current investigation revealed the presence of irregular-shaped protrusions extending from electron dense regressing ciliated cells. Apart from the prominent apical protrusions, the presence of condensed cytoplasm,

as well as nuclei with chromatin aggregation and margination were the major ultrastructural features which identified these electron dense ciliated cells as apoptotic. These characteristic features of apoptosis have been observed in the endometrial epithelium of the hamster (Sandow *et al*., 1979), cat (Verhage *et al.,* 1984) and human (Amso *et al*., 1994) in relation to hormonal fluctuations associated with either the menstrual or oestrous cycles. Additionally, an increase in the number of apoptotic cells has been detected in the oviduct of the domestic fowl during moulting (Heryanto *et al*., 1997), a period which is known to coincide with low circulating levels of luteinizing hormone, oestrogen and progesterone (Sundaresan *et al*., 2008).

Deciliation via cilia packet formation and release was a further notable feature of degenerating electron dense ciliated cells in the present study. The multi-ciliary composition of cilia packets was revealed with both transmission and scanning electron microscopy. The formation and extrusion of cilia packets has been described in the rat (Reeder and Shirley, 1999), opossum (Wick and Kress, 2002) and isthmic region of the domestic fowl (Mpango and Madekurozwa, 2018). Cilia packet formation in the rat (Reeder and Shirley,1999) was observed during all phases of the oestrous cycle except metestrus, while the presence of these ciliary structures in the opossum occurred in late estrus (Wick and Kress, 2002). These investigations suggested that cilia packet formation may be influenced by circulating levels of reproductive hormones.

In the present study degenerating electron lucent ciliated cells contained dilated RER cisternae, swollen mitochondria and cytoplasmic vacuoles. These ultrastructural features are characteristic of necrotic cell death (Majno and Joris, 1995; Trump *et al*., 1997). Additionally, the necrotic ciliated cells contained degenerating lipid droplet autophagosomes, which were indicative of fatty degeneration. In the dog, fatty

degeneration was observed in endometrial epithelial cells during late metoestrus and early anoestrus, which are stages of the oestrous cycle associated with decreasing levels of progesterone and oestradiol (Galabova *et al*., 2003).

Mitochondrial cells

The presence of mitochondrial cells has only been reported in the luminal epithelium of the avian isthmus and shell gland (Draper *et al*., 1972; Wyburn *et al*., 1973; Solomon, 1975; Mpango and Madekurozwa, 2018). Although mitochondrial cells were first described in the shell glands of the domestic fowl over forty years ago (Wyburn *et al*., 1973), the function of these cells is still unknown.

The ultrastructure of the mitochondrial cells in the present investigation was in general agreement with the findings of a study conducted by Wyburn *et al*. (1973). Mitochondrial cells in moulting hens used in the current study underwent autophagy in the earlier stages of regression and apoptosis in the more advanced degenerative phases. The consequences of these degenerative processes are unknown, largely because the function of mitochondrial cells is still unclear.

Acknowledgements

The authors acknowledge the assistance of University of Pretoria technical staff: Lizette du Plessis, Antoinette Lensink (Electron Microscope unit, Onderstepoort campus) and Erna van Wilpe (Laboratory for Microscopy and Microanalysis, Hatfield campus). The University of Pretoria is gratefully acknowledged for the MSc

postgraduate bursary awarded to Mike Mpango. This study was funded by the National Research Foundation of South Africa (grant #N00188).

Data availability statement

The data that support the findings of this study are available on request from the corresponding author. The data are not publicly available due to ethical restrictions.

References

Amso, N.N., S. Crow, J. lewin, R.W. Shaw, 1994: A comparative morphological and ultrastructural study of endometrial gland and fallopian tube epithelia at different stages of the menstrual cycle and the menopause. Human Reprod. **9,** 2234-2241.

Bar, A., 2009: Calcium transport in strongly calcifying laying birds: mechanism and regulation. Comp. Biochem. and Physiol. Part A. **152,** 447-469.

Biazik, J., P. Yla-Anttila, H. Vihinen, E. Jokitalo, E-L. Eskelinen, 2015: Ultrastructural relationship of the phagosome with surrounding organelles. Autophagy. **11,** 439-451.

Breen, P.C., P.P.H. De Bruyn, 1969: The fine structure of the secretory cells of the uterus (shell gland) of the chicken. J. Morphol. **128,** 35-66.

Chousalkar, K.K., J.R. Roberts, 2008: Ultrastructural changes in the oviduct

of the laying hen during the laying cycle. Cell Tiss. Res. **332,** 349-358.

Draper, M.H., M.F. Davidson, G.M. Wyburn, H.S. Johnston, 1972: The fine structure of the fibrous membrane forming region of the isthmus of the oviduct of *Gallus domesticus*. Quart. J. Exp. Physiol. **57,** 297-309.

Edinger, A.L., C.B. Thompson, 2004: Death by design: apoptosis, necrosis and autophagy. Curr. Opinion Cell Biol. **16,** 663-669.

Elmore, S., 2007: Apoptosis: a review of programmed cell death. Toxicol. Path. **35,** 495-516.

Eroschenko, V.P., W.O. Wilson, 1974: Histological changes in the regressing reproductive organs of sexually mature male and female Japanese quail. Biol. Reprod. **11,** 168-179.

Fiers, W., R. Beyaert, W. Declercq, P. Vandenabeele, 1999: More than one way to die: apoptosis, necrosis and reactive oxygen damage. Oncogene. **18,** 7719-7730.

Fernandez, M.S., C. Escobar, I. Lavelin, M. Pines, J.L. Arias, 2003: Localization of osteopontin in oviduct tissue and eggshell during different stages of the avian egg laying cycle. J. Struct. Biol. **143,** 171-180.

Galabova, G., M. Egerbacher, J.E. Aurich, M. Leitner, I. Walter, 2003: Morphological changes of the endometrial epithelium in the bitch during metoestrus and anoestrus. Reprod. Dom. Ani. **38,** 415-420.

Gautron, J., M.T. Hincke, K. Mann, M. Panheleux, M. Bain, M.D. Mckee, S.E. Solomon, Y. Nys, 2001a: Ovocalyxin-32, a novel chicken eggshell matrix protein. J. Biol. Chem. **42,** 39243-39252.

Gautron, J., M.T. Hincke, K. Mann, M. Panheleux, J.M. Garcia-Ruiz, T. Boldicke, T. Nys, 2001b: Ovotransferrin is a matrix protein of the hen eggshell membranes and basal calcified layer. Conn. Tiss. Res. **42,** 255-267.

Gupta, S.K., B.R. Maiti, 1987: Seasonal changes in the oviduct of the pied myna (aves: *sturnidae*). J. Morphol. **194,** 247-263.

Hargitai, R., N. Boross, S. Hamori, E. Neuberger, Z. Nyiri, 2017: Eggshell biliverdin and protoporphyrin pigment in a songbird: are they derived from erythrocytes, blood plasma or the shell gland. Physiol. Biochem. Zool. **90,** 613-626.

Heryanto, B., Y. Yoshimura, T. Tamura, T. Okamoto, 1997: Involvement of apoptosis and lysosomal hydrolase activity in the oviductal regression during induced moulting in chickens: a cytochemical study for end labelling of fragmented DNA and acid phosphatise. Poult. Sci. **76,** 67-72.

Hincke, M.T., C.P. Tsang, M. Courtney, V. Hill, R. Narbaitz, 1995: Purification and immunochemistry of a soluble matrix protein of the chicken eggshell (ovocleidin 17). Cal. Tiss. International. **56,**578-583.

Johnston, H.S., R.N.C. Aitken, G.M. Wyburn, 1963: The fine structure of the uterus of the domestic fowl. J. Anat. **97,** 333-344.

Jonchere, V., A. Brionne, J. Gautron, Y. Nys, 2012: Identification of uterine ion

transporters for mineralisation precursors of the avian eggshell. BMC Physiol. **12,** 10.

Kerr, J.F.R., A.H. Wyllie, A.R. Currie, 1972: Apoptosis: a basic biological phenomenon with wide ranging implications in tissue kinetics. Brit. J. Cancer. **26,** 239-257.

Madekurozwa, M.-C., 2007: Ultrastructural features of the uterus in the sexually immature ostrich (*Struthio camelus*) during periods of ovarian inactivity and activity. Onder. J. Vet. Res. **74,** 209-216.

Madekurozwa, M.-C., 2013: An immunohistochemical study of the oviduct in the domestic fowl (*Gallus domesticus*). Anat. Histol. Embryol. **42,** 48-56.

Madekurozwa, M.-C., 2014: Immunolocalization of intermediate filaments and laminin in the oviduct of the immature and mature Japanese quail (*Coturnix coturnix japonica*). Anat. Histol. Embryol. **43,** 210-220.

Majno, G., I. Joris, 1995: Apoptosis, oncosis and necrosis: an overview of cell death. Am. J. Path. **146,** 3-15.

Mpango, M.M., M.-C. Madekurozwa, 2018: Comparative histomorphological and ultrastructural study of the luminal epithelium of the isthmus in laying and moulting domestic fowls (*Gallus domesticus*). Anat. Histol. Embryol. **47,** 444-455.

Rahman, M.A., A. Moriyama, B.A. Iwasawa, N. Yoshizaki, 2009: Cuticle formation in

quail eggs. Zool. Sci. **26,** 496-499.

Reeder, R.L., B. Shirley, 1999: Deciliation in the ampulla of the rat oviduct and effects of estrogen on the process. J. Exp. Zool. **283,** 71-80.

Robinson, D.S., N.R. King, D.J. Bowen, 1968: The occurrence of neutral and acidic mucins in the reproductive tract of the laying hen. Histochemie. **13,** 97-104.

Sanchez-Wandelmer, J., N.T. Ktistakis, F. Reggiori, 2015: ERES: sites for autophagosome biogenesis and maturation? J. Cell Sci. **128,** 185-192.

Sandow, B.A., N.B. West, R.L. Norman, R.M. Brenner, 1979: Hormonal control of apoptosis in hamster uterine luminal epithelium. Am. J. Anat. **156,** 15-36.

Sato, T., Y. Fukazawa, H. Kojima, M. Enari, T. Iguchi, Y. Ohta, 1997: Apoptotic cell death during the estrous cycle in the rat uterus and vagina. Anat. Rec. **248,** 76-83.

Solomon, S.E., 1975: Studies on the isthmus region of the domestic fowl. Brit. Poult. Sci. **16,** 255-258.

Spornitz, U.M., B.P. Rinderknecht, A. Edelmann, B. Scheidegger, F. Cairoli, 1994: Ultrastructure as a basis for dating of rat endometrium. Anat. Rec. **238,** 163-176.

Sundaresan, N.R., D. Anish, K.V.H. Sastry, V.K. Saxena, K. Nagarajan, J. Subramani,

M.D.M. Leo, N. Shit, J. Mohan, M. Saxena, K.A. Ahmed, 2008: High doses of dietary zinc induce cytokines, chemokines and apoptosis in reproductive tissues during regression. Cell Tiss. Res. **332,** 543-554.

Trump, B.F., I.K. Berezesky, S.H. Chang, P.C. Phelps, 1997: The pathways of cell death: oncosis, apoptosis and necrosis. Toxicol. Path. **25,** 82-88

Verhage, H.G., M.K. Murray, R.A. Boomsma, R.A. Rehfeldt, R.C. Jaffe, 1984: The postovulatory cat oviduct and uterus: correlation of morphological features with progesterone receptor levels. Anat. Rec. **208,** 521-531.

Wasserman, R.H., C.A. Smith, C.M. Smith, M.E. Brindak, C.S. Fullmer, L. Krook, J.T. Penniston, 1991: Immunohistochemical localization of a calcium pump and calbindin-D_{28k} in the oviduct of the laying hen. Histochem. **96,** 413-418.

Wick, R., A. Kress, 2002: Ultrastructural changes in the uterine luminal and glandular epithelium during the oestrous cycle of the marsupial *Monodelphis domestica* (grey short-tailed opossum). Cells Tiss. Org. **170,** 111-131.

Williams, T.D., C.E. Ames, 2004: Top-down regression of the avian oviduct during late oviposition in a small passerine bird. J. Exp. Biol. **207,** 263-268.

Wilson, P.W., C.S. Suther, M.M. Bain, W. Icken, A. Jones, F. Quinlan-Pluck, V. Olori, J. Gautron, I.C. Dunn, 2017: Understanding avian egg cuticle formation in the oviduct: a study of its origin and deposition. Biol. Reprod. **97,** 39-49.

Wyburn, G.M., H.S. Johnston, M.H. Draper, M.F. Davidson, 1973: The ultrastructure

of the shell forming region of the oviduct and the development of the shell of *Gallus domesticus*. Quart. J. Exp. Physiol. **58,** 143-151.

Yamamoto, T., H. Ozawa, H. Nagai, 1985: Histochemical studies of Ca-ATPase, succinate and NAD^+-dependent isocitrate dehydrogenases in the shell gland of laying Japanese quail: with special reference to calcium-transporting cells. Histochem. **83,** 221-226.

Yu, J.Y.L., R.R. Marquardt, 1974: Hyperplasia and hypertrophy of the chicken (*Gallus domesticus*) oviduct during a reproductive cycle. Poult. Sci. **53,** 1096-1105.

Zeiss, C.J., 2003: The apoptosis-necrosis continuum: insights from genetically altered mice. Vet. Path. **40,** 481-495.

Zhao, R., G.Y. Xu, Z.Z. Liu, J.Y. Li, N. Yang, 2006: A study on eggshell pigmentation: biliverdin in blue-shelled chickens. Poult. Sci. **85,** 546-549.